ACS NANO

www.acsnano.org

ARTICLE

A Wulff in a Cage: The Confinement of Substrate-Based Structures in Plasmonic Nanoshells, Nanocages, and Nanoframes Using Galvanic Replacement

Maryam Hajfathalian, Kyle D. Gilroy, Spencer D. Golze, Ali Yaghoubzade, Eredzhep Menumerov, Robert A. Hughes, and Svetlana Neretina*

College of Engineering, Temple University, Philadelphia, Pennsylvania 19122, United States

Supporting Information

ABSTRACT: Galvanic replacement reactions carried out on solid core−shell structures typically yield a noble metal nanorattle geometry in which a mobile core is contained within a hollowed shell. Here, we adapt this colloidal synthesis to substrate-based structures to obtain a fundamentally altered product in which an immobilized core is separated from the shell by a well-defined gap, an architecture unobtainable using colloidal techniques and that offers unique advantages in terms of generating plasmonic near-field effects within the confines of a single structure. In the devised route, Wulff-shaped templates of Au, Pt, or Pd, formed through the dewetting of ultrathin films, are first transformed into core−shell structures through the reduction of Ag^+ ions onto their surface and then further transformed through the galvanic replacement of Ag with Au. Through suitable adjustments to the shell geometry, the epitaxial relationship with the substrate, and the extent to which the shell is replaced, it is possible to generate an entire family of nanostructures in which a Wulff-shaped core is confined within a nanoshell, nanocage, or nanoframe, where, in all cases, bonds formed between the structure and the substrate preclude motion. With the potential to tune the gap width, the geometry of the confining structure, and the composition of the core, shell, and substrate, these structures could find application as catalytic nanoreactors able to drive both single-step and cascade reactions or as plasmon-based sensing elements for biological and chemical detection.

KEYWORDS: *nanoshell, nanocage, nanoframe, core−shell, galvanic replacement, plasmon*

Downloaded via UNIV OF NOTRE DAME on July 28, 2021 at 19:58:15 (UTC).
See https://pubs.acs.org/sharingguidelines for options on how to legitimately share published articles.

Template-mediated solution-based chemistry has proven to be one of the most effective means for exerting architectural control over syntheses directed toward the formation of complex noble metal nanostructures.[1−5] Such syntheses aim to replace erratic and disorganized self-nucleation processes with orderly processes dictated by well-defined templates capable of exerting control over reaction pathways such that a single end-product is produced in high yield. Templates can act as platforms upon which material is deposited or sculpted through its partial dissolution into the adjacent liquid medium. These additive and subtractive processes can also be used in combination to yield a product displaying even greater intricacy. The template itself can be completely eliminated from the final structure, become partially hollowed, or be assimilated into the end-product intact or as a chemically altered material. In all cases, the objective is to obtain nanostructure architectures with properties and functionalities unrealizable through other means. Such nanomaterials are of high relevance to sensing,[6] catalytic,[7,8] photovoltaic,[9] and biomedical applications.[10]

Through the use of reduction−oxidation (redox) reactions it is possible to activate both additive and subtractive template-mediated growth modes. The heterogeneous nucleation of reduced metal ions onto the template, for example, provides a straightforward strategy for obtaining bimetallic core−shell structures (abbreviated as core@shell).[11,12] Shape control can be achieved by suitably adjusting the kinetics of the deposition process[13−15] or through the deployment of facet-selective capping agents able to promote the advancement of specific facets.[3,16] Tunable nanostructure properties are realized by varying the overall shape of the structure, the thickness of the shell, and/or the metals which make up the core and shell. Galvanic replacement reactions also rely on redox chemistry,

Received: April 22, 2016
Accepted: May 12, 2016
Published: May 12, 2016

© 2016 American Chemical Society

DOI: 10.1021/acsnano.6b02712
ACS Nano 2016, 10, 6354−6362

but where material is simultaneously added and subtracted from a template as it undergoes a dramatic transformation in composition and morphology.[1] These reactions are driven by favorable differences in the redox potential between the template and the metal ions in the precursor solution. If the metal ions have a more positive redox potential than the template, then they become reduced and plate the surface of the template as template atoms become oxidized and dissolve into solution. The overall process is quite involved, first transforming a solid template into a hollow shell, then into a caged structure exhibiting substantial openings on its side facets, and finally into a mere frame where material exists only along the ridges where the template facets originally met. This morphological evolution is accompanied by changes to the composition, which trend from that of the template metal, to an alloyed shell, to a dealloyed nanocage, to a nanoframe composed almost entirely of the reduced metal. Because galvanic replacement reactions can be terminated at any point along the reaction pathway, it is possible to derive an entire family of nanostructure architectures from a single synthetic protocol. As a result, noble metal nanoshells,[1] nanocages,[17] and nanoframes[2,18,19] are all attractive in that they have distinctive properties that can be tuned over a wide parameter space. By combining the two aforementioned procedures, nanostructures of even greater structural complexity are obtained when galvanic replacement reactions are carried out on core−shell structures. In a scenario where the shell, but not the core, is subject to replacement, the reaction product is a shell that encapsulates a mobile core and an adjacent void (*i.e.*, core@void@shell). Such structures, referred to as nanorattles, were first synthesized by Xia and co-workers[20,21] and have since been demonstrated for numerous geometries and materials.[22−27]

In a series of reports, we have demonstrated template-mediated solution-based syntheses as being amenable to adaptations that allow them to be carried out on templates that are immobilized on the surface of a substrate.[28−33] The strategy is reliant on the fabrication of seeds through the dewetting of ultrathin metal films.[34] Such seeds are free of ligands, can form a heteroepitaxial relationship with the substrate, and, for metals with a face centered cubic crystal structure, adopt the equilibrium Wulff shape[35] (*i.e.*, a truncated octahedron enclosed by six square {100} facets and eight hexagonal {111} facets). The heterogeneous nucleation of Ag onto Wulff-shaped Au templates has resulted in the synthesis of substrate-based Au@Ag nanocubes,[28] octahedra,[29] and truncated octahedra.[29] Galvanic replacement reactions performed on Ag templates have resulted in the formation of substrate-based AuAg nanoshells and nanocages.[30,31] Together, these syntheses provide the procedures needed to adapt the nanorattle strategy to substrate-immobilized templates. Here, we carry out such a strategy using substrate-immobilized X@Ag (X = Au, Pt, Pd) core−shell structures and obtain Wulff-shaped nanostructures confined within AuAg nanoshells, nanocages, and nanoframes. In stark contrast to nanorattles, where the mobile core rests against the confining nanoshell, the substrate-based structures maintain a well-defined gap between the inner core and outer shell since both of these components are immobilized by the underlying substrate. It is the formation of this gap, a property that is unrealizable using solution-dispersed templates, that could act as an enabler for advancing functional surfaces of plasmonic and chemically active noble metal nanostructures.

RESULTS

The Reaction Scheme. The devised procedure for confining a Wulff-shaped Au nanostructure within a nanoshell, nanocage, or nanoframe is shown schematically in Figure 1.

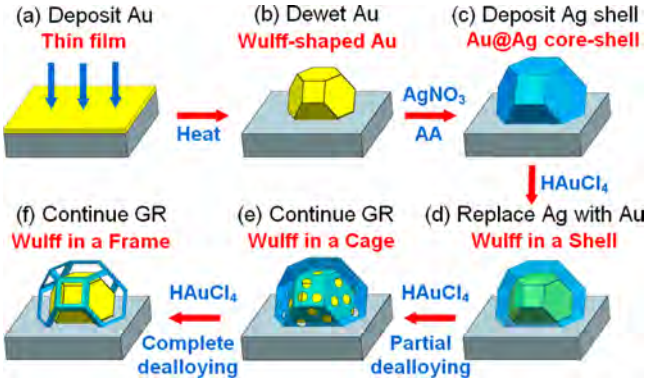

Figure 1. Schematic showing the synthetic procedure for forming nanoshells, nanocages, and nanoframes around Wulff-shaped Au nanostructures that are substrate-immobilized. The procedure involves (a) the deposition of an ultrathin Au film, (b) its assembly into Au templates through thermal dewetting, (c) the formation of a solid Ag shell around the template through the reduction of Ag^+ by ascorbic acid (AA), (d) the galvanic replacement (GR) of Ag with Au to form a AuAg nanoshell, and (e) the dealloying of the nanoshell to transform it into a nanocage and (f) nanoframe.

This multistage synthesis begins with the physical vapor deposition of an ultrathin layer of Au (Figure 1a). The film is then heated in an inert atmosphere to temperatures that induce dewetting while providing sufficient energy for the island-shaped nanostructures to assume the equilibrium Wulff shape and form a heteroepitaxial relationship with the crystalline substrate (Figure 1b). It is noted that surface energy considerations typically demand a truncation of the Wulff shape at the substrate−nanostructure interface, the extent of which is material-dependent.[35] The substrate-immobilized Au templates are then immersed into a heated aqueous solution containing a reducing agent (*e.g.*, ascorbic acid) into which aqueous $AgNO_3$ is injected. The ensuing reaction reduces Ag^+ ions to Ag^0, a neutral species that readily deposits on the Au templates to form a Au@Ag core−shell structure (Figure 1c). A galvanic replacement reaction is then carried out on the Ag shell by exposing these structures to aqueous $HAuCl_4$. As Au^{3+} ions react with the Ag template, they become reduced to Au^0 and plate its surface. Alloying between the plated Au and Ag template leads to the formation of a AuAg shell, but where continued deposition causes it to become increasingly Au-rich and, hence, relatively impervious to further Ag oxidation. At this stage, oxidation mostly occurs through template hollowing from a single opening in the shell through which oxidized Ag is removed as Au is continuously deposited on the surface of the shell. This process continues until the supply of pure Ag is exhausted, after which the opening seals.[36,37] If, at this stage, the reaction is halted through the removal of the substrate from the reaction vessel, then the Wulff-shaped Au is encapsulated in a continuous AuAg nanoshell where the shell and core are separated by a gap (Figure 1d). If, however, the galvanic replacement reaction is allowed to proceed, then the AuAg shell dealloys as more Au^{3+} is reduced onto the shell as Ag^+ ions exit from its surface. The dealloying process triggers a morphological reconstruction of the shell due to an overall loss of

DOI: 10.1021/acsnano.6b02712
ACS Nano 2016, 10, 6354−6362

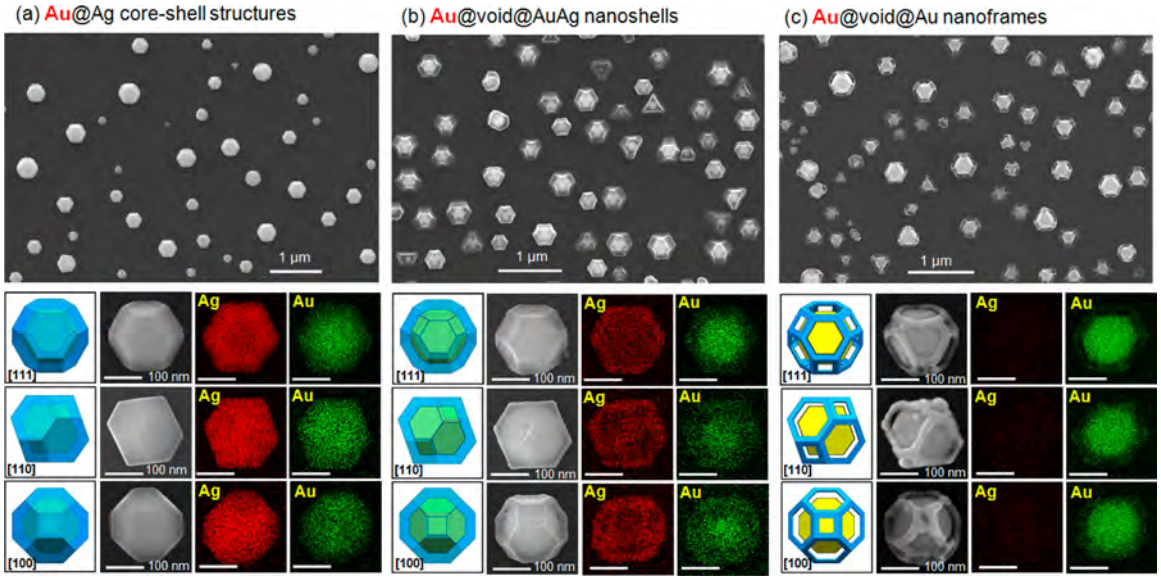

Figure 2. Plan view SEM images for substrate-based nanostructures with the (a) Au@Ag core−shell, (b) Au@void@AuAg nanoshell, and (c) Au@void@Au nanoframe configurations. For all cases, schematics and elemental maps are shown for individual nanostructures derived from Au templates having the [111]-, [110]-, and [100]-axes normal to the substrate surface.

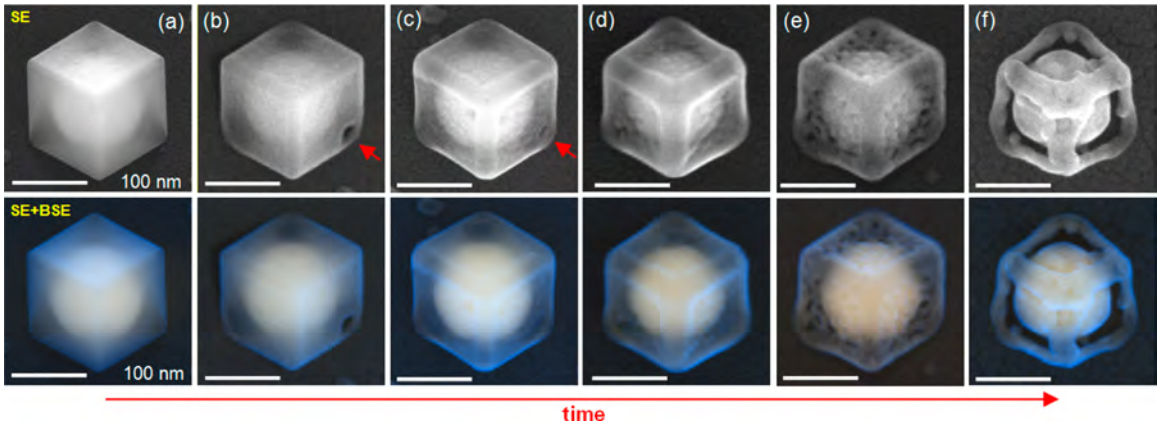

Figure 3. Plan view SEM images (top row: SE mode, bottom row: SE + BSE mode) showing the evolution of a [111]-oriented Au@Ag nanocube as the Ag shell undergoes galvanic replacement.

material resulting from the 3:1 Ag^{+}:Au^{3+} replacement ratio.[1] Eventually, the material loss is sufficient to cause the side facets most prone to dealloying to rupture in numerous locations, a process that, if terminated, results in a product with the nanocage configuration (Figure 1e). Continued dealloying leads to the disintegration of the facet faces, eventually leaving behind a framework that traces out the seams where the Ag shell facets once met. A reaction halted at this stage results in an Au core encircled by a near-pure Au nanoframe (Figure 1f).

Nanostructure Synthesis Using Au Templates. Figure 2 shows plan view scanning electron microscopy (SEM) images and the associated elemental maps for structures obtained when terminating the synthesis at various points in the reaction scheme. The predominantly [111]-oriented Au templates used in the syntheses were formed on [0001]-oriented sapphire substrates in one of two epitaxial relationships given by $(111)[-211]_{Au}\|(0001)[11-20]_{sapphire}$ and $(111)[2-1-1]_{Au}\|(0001)$-$[11-20]_{sapphire}$.[38] Smaller yields of [110]- and [100]-oriented templates are also formed and are monitored in this study so as to track the evolution of all three low-index orientations. The overgrowth of Ag on these templates results in the Au@Ag core−shell structures shown in Figure 2a. For the most part, the solid Ag shells form a conformal layer for all template orientations, but where it should be understood that the growth kinetics were adjusted to achieve this outcome.[29] When deviations from conformal growth are observed, it is typically for smaller templates and leads to the formation of triangular-shaped core−shell structures due to the preferential growth of (111) facets. The galvanic replacement of the Ag shell by Au^{3+} ions leads to the formation of the Au@void@AuAg nanoshells shown in Figure 2b. The reaction product appears as a downward-facing faceted shell that, in combination with the underlying substrate, envelopes the Au core. Bonds formed between the shell and the substrate during the replacement reaction ensure shell adhesion and the preservation of a well-defined gap between it and the core. At this stage, the predominantly Au shells are weakly alloyed with Ag and can show low levels of porosity. The smooth morphologies exhibited by the galvanic replacement of this solution-grown Ag contrast with the rough morphologies exhibited when templates are formed through the dewetting of Ag films,[31] a fact that suggests that fundamental differences may exist between

DOI: 10.1021/acsnano.6b02712
ACS Nano 2016, 10, 6354−6362

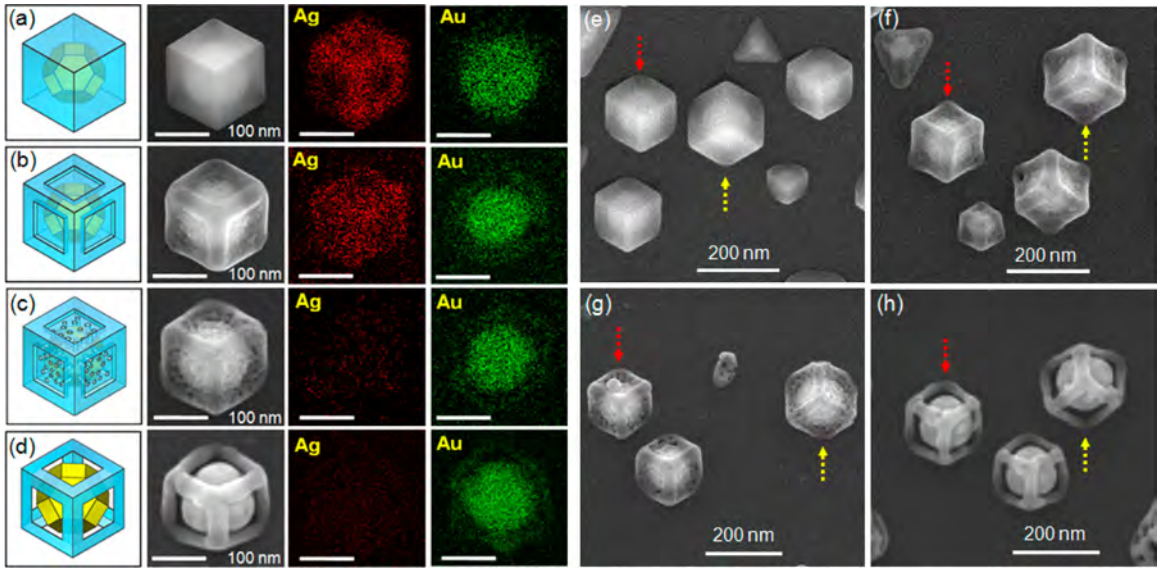

Figure 4. Schematics, SEM images, and elemental maps of a cube-shaped nanostructure with a (a, e) core−shell, (b, f) nanoshell, (c, g) nanocage, and (d, h) nanoframe configuration.

templates formed using these two methods. Dealloying Ag from the shells causes many pores to open up on the facets (Supporting Information, Figure S1), which, over time, grow and merge to form the nanoframes shown in Figure 2c. These structures, regardless of orientation, show prominent openings where the (111) facets of the shell once existed. Openings also appear on the (100) facets, but to a lesser extent. Elemental mapping indicates that both the core and frame are composed of Au, with no detectable levels of Ag. If the structures are reacted further, the framework weakens, eventually causing it to collapse onto the inner core and/or have fragments released into the adjacent liquid (Supporting Information, Figure S2). Such a process is consistent with the fragmentation process that occurs when solution-dispersed templates are overreacted.[1]

Through the use of facet-selective capping agents it is possible to redirect the synthesis of the Ag shell toward core−shell architectures that are different from those shown in Figure 2a and, in doing so, fundamentally alter the product realized when carrying out the reaction scheme. Recently, we demonstrated a two-reagent synthesis in which Ag^+ is reduced onto substrate-immobilized Au templates using citrate as the reductant and capping agent.[28] The reaction product is a Wulff-shaped Au core enclosed within a Ag shell shaped as a (100)-faceted nanocube. Figure 3 presents a series of plan view SEM images that show the time evolution of a [111]-oriented Au@Ag nanocube as the Ag shell undergoes galvanic replacement. The images are shown as both secondary electron (SE) and mixed mode images, where the latter combines the secondary and backscattered electron (BSE) images in a manner that accentuates the core−shell geometry. The progression shows many of the same features observed when solution-dispersed nanocubes undergo galvanic replacement reactions.[36] The initial stages of the reaction see the heteroepitaxial deposition of Au onto the shell and the formation of a single opening that acts as a portal through which oxidized Ag^+ is released from the shell interior (Figure 3b). When the supply of pure Ag is exhausted, the pit closes to form a nanoshell (Figure 3c,d). Shell dealloying results in further Au deposition and the formation of highly porous sidewalls (Figure 3e), which eventually give way to the nanoframe configuration where substrate immobilization, once again, results in a well-defined gap between the Wulff-shaped Au core and the surrounding frame (Figure 3f). For this case, however, the well-defined openings form on the (100) facets. Figure 4 shows SEM images and the associated elemental maps of individual structures formed at points of significance in the reaction sequence as well as corresponding images of surfaces containing many of these same structures. The elemental maps confirm that the box-shaped nanoshell (Figure 4b) is composed of a AuAg alloy and that there is a near-total loss of Ag for the nanoframe (Figure 4d). It is also evident from the images that identical structures form in one of two possible crystallographic orientations relative to the underlying substrate (denoted by the red and yellow arrows in Figures 4e−h).

While the galvanic replacement of these substrate-based structures shows obvious parallels to the corresponding solution-based growth modes, there are differences. Most notable is the tendency for preferential deposition to occur on the ridges of the nanocube. As a result, the ridges become increasingly exaggerated over the course of the replacement reaction (Figure 3b−d), leaving the (100) facets exceedingly thin. This difference carries over to the early stages of the dealloying phase, causing the (100) facets to rupture in numerous locations to form a thin permeable mesoporous membrane on each of the sidewalls having a lace-like appearance (Figure 4c). With rounded ridges and perforated facets, these large surface area nanocages must have both a large surface energy and a high density of atomic steps, kinks, and undercoordinated atoms. While the appearance of many pores on dealloyed facets is not unique to this work,[39] the overall structure is without precedent. These differences could originate from the fact that our nanocube synthesis does not utilize poly(vinylpyrrolidone) as a capping agent as is typically the case. It also noted that the total mass of the Au templates (0.6 μg) is significantly smaller than is typically used in colloidal syntheses, a factor that could significantly alter growth kinetics.

Optical Characterization. Accompanying the extensive morphological transformations occurring over the course of the reaction sequence are equally dramatic changes to the optical properties. Figure 5 shows the evolution of the extinction

DOI: 10.1021/acsnano.6b02712
ACS Nano 2016, 10, 6354−6362

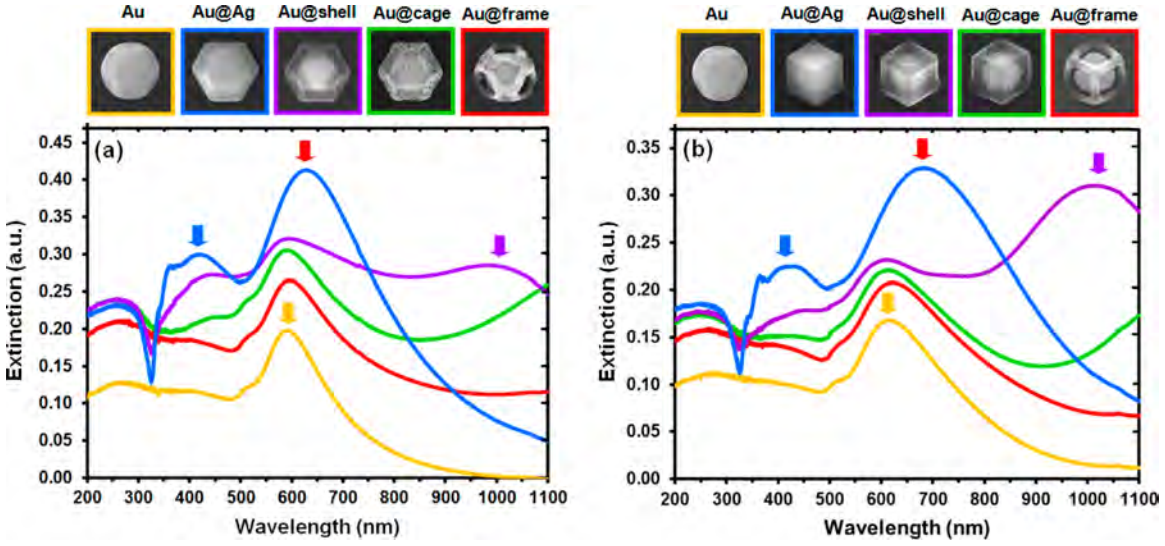

Figure 5. Extinction spectra for the various nanostructures formed as Au templates are transformed into Au@Ag core−shell structures and then undergo galvanic replacement to achieve Wulff-shaped Au nanostructures confined within a nanoshell, nanocage, and nanoframe. The two plots compare spectra obtained when the reaction scheme is directed along a path yielding confining structures with a (a) truncated octahedron and (b) cubic geometry.

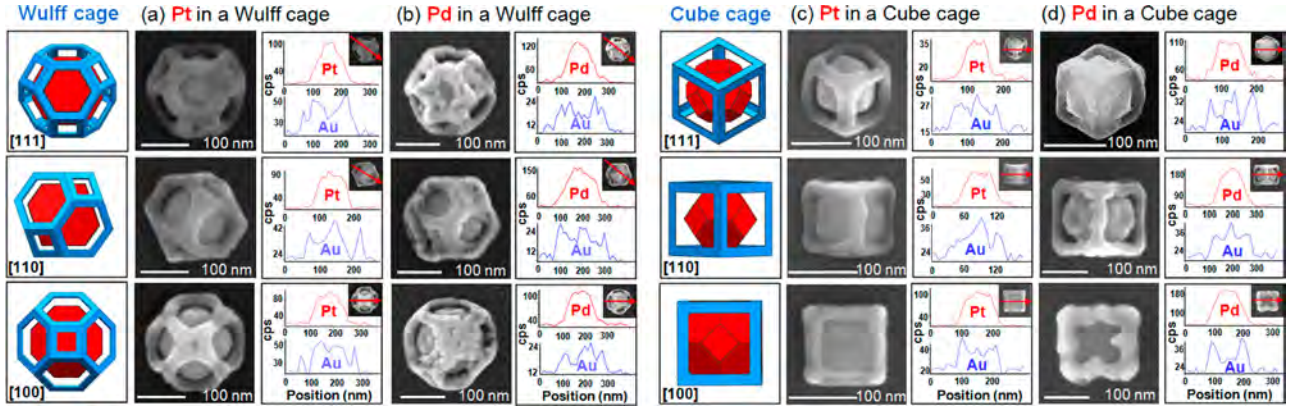

Figure 6. Schematics, SEM images, and elemental line scans for nanoframes obtained when the shells of (a) Pt@Ag and (b) Pd@Ag structures with a truncated octahedron geometry and (c) Pt@Ag and (d) Pd@Ag structures with a cubic geometry are galvanically replaced with Au. For each case, structures are shown that are derived from [111]-, [110]-, and [100]-orientated templates.

spectra that occurs as Au@Ag core−shell structures with truncated octahedron and cubic geometries progress through the various stages of the reaction scheme. With each stage of the reaction giving rise to a profoundly altered response there is the opportunity to tune the optical properties to a desired specification. At the same time, it should be recognized that, as plasmonic materials, the optical behavior is highly complex, involving not only fundamental changes to the nanostructure shape, size, and composition, but where coupling phenomena are possible and where structures are exposed to the asymmetric dielectric environment resulting from the adjacent substrate. While simulations of the optical response over the entire course of the reaction have proven to be a formidable challenge, the overall behavior follows trends similar to those observed when plasmonic noble metal colloids undergo comparable morphological transformations.

A comparison of the extinction spectra obtained using Au@Ag core−shell structures with truncated octahedron (Figure 5a) and cubic (Figure 5b) geometries indicates that the overall trends are quite similar. Each is derived from Au templates that exhibit a prominent plasmon resonance near 600 nm (denoted by the yellow arrow) with a shoulder at 520 nm, as is expected for a Wulff-shaped structure.[40,41] The addition of a Ag shell to these templates results in an overall increase in the extinction efficiency, a red shift in the primary plasmon peak (red arrow), and the emergence of a second plasmon mode centered near 420 nm (blue arrow) on which several smaller reproducible peaks are superimposed. The emergence of a second low-wavelength plasmon mode is in line with spectra obtained for rather thick shells formed on Au colloids.[12,42] The behavior has been modeled by Ma *et al.*[43] using simulations based on the discrete dipole approximation (DDA), which rationalize the spectral features through a hybridization of the plasmon resonances of the Au core and Ag shell. The transformation to a nanoshell morphology through galvanic replacement causes (i) a weakening of the primary plasmon mode, which is accompanied by a blue shift back to values near its original position (*i.e.*, 600 nm), (ii) the 420 nm mode to diminish in strength, and (iii) the emergence of a broad mode centered in the near-infrared (violet arrow). As the galvanic replacement reaction transforms the structures into nanocages and nanoframes, the near-infrared mode red shifts and the plasmon peak

DOI: 10.1021/acsnano.6b02712
ACS Nano 2016, 10, 6354−6362

centered near 600 nm increasingly takes on the character of the starting Au template. Such behavior is consistent with both the expected response from a nanoframe[2] and an inner core plasmon resonance that becomes increasingly decoupled from the confining structure. For all cases, the expected influence of the substrate is to red shift the plasmon modes.[44]

Nanostructure Synthesis using Pt and Pd Templates. Synthetic trials were also carried out in which the Au templates were substituted for Pt and Pd in the reaction scheme. Pt@Ag and Pd@Ag core−shell structures were first synthesized where the Ag shell took on both the truncated octahedron and cubic geometries. Figure 6 shows SEM images and elemental line scans obtained using (111)-, (110)-, and (100)-oriented templates after the Ag shell underwent galvanic replacement with Au to the extent that it was transformed into a nanoframe. For all cases, structures are formed that are analogous to those obtained using similarly oriented Au templates. These results demonstrate the viability of extending the synthetic strategy to other noble metal templates. In doing so, it expands the complexity of the structures obtainable in that the inner core of one metal is surrounded by a nanoframe of a second metal, where in all cases the core and frame are isolated from one another by a gap. While such results are promising, several concerns still remain. Foremost, is the fact that we have not yet achieved the same degree of synthetic control for these structures compared to those produced with Au templates. Many of the structures produced take on irregular geometries, indicating that the crystallographic properties of the template have not asserted the desired control over the reaction. A second concern stems from the fact that Au, because it has a higher electrochemical potential than Pt and Pd, could galvanically replace the core material. While the elemental line scans show no evidence that this is occurring to any significant degree over the duration of the synthesis, we cannot rule out the possibility that the core material is coated with a thin layer of Au.

DISCUSSION

The devised reaction scheme yields a never before realized family of nanostructures that allow for a high degree of chemical and architectural control to be exerted over the reaction product. Such nanostructure architectures, in many respects, seem ideal from the standpoint of exploiting the extraordinary optical and chemical properties exhibited by noble metal nanostructures. Properties of significance include (i) the ability to form a well-defined gap between the inner core and outer shell, (ii) a nanostructure interior composed of three materials (*i.e.*, the core, shell, and substrate), each of which has the potential to offer functionality, and (iii) tunable nanostructure architectures where the core material can be enclosed in a protective shell, connected to the outside environment through a mesoporous cage, or encircled by a frame offering near-complete exposure to the surroundings. By capitalizing on these features, we believe that there is the potential to realize functionalities that are unique to these nanomaterials or which outperform existing materials. In the remainder of this discussion section we outline how the overall synthetic strategy may be used to achieve such an outcome and, hence, highlight the potential significance of these substrate-based structures.

With chemical controls deciding nanostructure faceting, geometry, and composition and the synthesized nanostructures having large surface areas and a high density of atomic steps, kinks, and undercoordinated atoms, these nanostructures present intriguing possibilities from the standpoint of catalysis. The core@void@cage architecture, in particular, seems ideally suited as a nanoreactor able to catalyze reactions within the confines of the void space before releasing the reaction product to the outside environment. The chemical environment within such a nanoreactor would be unique in that it could house multiple noble metal catalysts as well as an oxide material (*i.e.*, the substrate). Yolk−shell architectures deploying oxide−metal combinations as catalysts have, in fact, been demonstrated for a wide variety of systems.[45−47] With proper design, such an environment could also promote cascade reactions whereby multiple catalysts drive multistep reaction sequences. With obvious efficiencies derived from such an approach, there is increasing attention being paid to nanoreactors capable of sustaining sequential catalytic processes.[48,49] The use of plasmonic materials provides further opportunity in that there is the potential to power these nanoscale reactors using plasmonic near-fields and/or the localized heating generated by plasmon decay.[50,51] Plasmonic structures provide further benefit in that their spectral dependencies are highly tunable.

Substrate-based nanomaterials provide a natural platform for integration into sensing devices. With a scope of potential interactions stemming from plasmonic heating or near-fields, hot electron injection into adjacent mediums, a sensitivity to the surrounding dielectric environment, and the ability to catalytically transform chemical species, noble metal nanostructures provide a wide range of modalities on which to base sensors. Nanostructures of the type demonstrated in the current study will inevitably share many of the same advantages exhibited by other noble metal nanostructures such as the tunability of plasmonic resonances, shape- and facet-engineering, easily functionalized surfaces, and the ability to host guest molecules either within the void space or through surface conjugation. The core@void@shell architecture, however, has the potential to achieve an additional degree of tunability if synthetic control can be exerted over the width of the void. Such a capability would allow for a coupled response between the core and shell, which could be intensified or diminished in a controllable manner. The intense interest in dimer structures is, in fact, a direct consequence of the coupling phenomenon achieved through nanogap engineering.[52] Sensing modes could also rely on structures where a shell made of one material acts as the analyte receptor, while the plasmonic core of a second material acts as the sensing element. Structures could also be designed where there exists near-field hot spots within the void space, providing an excellent environment for detection modes reliant on surface enhanced Raman scattering (SERS).[6] Such structures should also be amenable to detection strategies based on colorimetric changes or plasmon-enhanced fluorescence.[6] These same detection strategies could be further augmented if templates are first formed in periodic arrays,[28−30,53,54] allowing for better monodispersity and opening up the possibility of fabricating pixelated sensing devices.

CONCLUSION

The study carried out advances an area of research that aims to integrate many of the competencies of colloidal chemistry with substrate-based techniques. By adapting the nanorattle protocol to the substrate-based platform we have generated a class of hollowed nanomaterials confined in a nanoshell, nanocage, or nanoframe configuration where the internal environment is characterized by a Wulff-shaped noble metal nanostructure

DOI: 10.1021/acsnano.6b02712
ACS Nano 2016, 10, 6354−6362

isolated from the confining structure by a well-defined gap and the supporting substrate material. These syntheses yield what are arguably the most complex noble metal nanostructures ever obtained when carrying out solution-based growth modes on substrate-based templates. With the potential for a coupled response between the core, shell, and substrate components, there is the potential to advance chemically and optically active surfaces for catalytic and sensing applications.

EXPERIMENTAL SECTION

Chemicals. Sputter targets of Au, Pt, and Pd were cut from 0.5 mm thick foils (Alfa Aesar) with purity levels of 99.9985%, 99.99%, and 99.95%, respectively, while the Bi target was cut from a rod with 99.999% purity (ESPI Metals). Two-side polished sapphire substrates with dimensions of 7 × 7 × 0.5 mm were cleaved from 3 in. diameter wafers (MTI Corporation). Dewetting procedures utilized ultra-high-purity Ar as the processing gas. Template-mediated syntheses were carried out using 99.9999% silver nitrate (Sigma-Aldrich), hydrogen tetrachloroaurate(III) trihydrate (Alfa Aesar), 99% L-ascorbic acid (Fisher Scientific), 99% trisodium citrate dihydrate (Alfa Aesar), and nitric acid (Sigma-Aldrich). All solution-based syntheses were carried out using deionized (DI) water with a resistivity of 18.2 MΩ·cm, where the glassware was cleaned with *aqua regia* and rinsed with DI water prior to use. All chemicals were used as received.

Template Preparation. The procedures used to obtain template materials are described in detail elsewhere.[55,56] In all cases, template formation proceeded through the dewetting of ultrathin films that were sputter deposited onto [0001]-oriented sapphire substrates. For the case of Pt, the dewetting was enhanced using a sacrificial layer of Bi.[56] Pt templates were exposed to dilute *aqua regia* (5 mM, molar ratio HCl:HNO_3 is 3:1) for 5 s and then rinsed in DI water immediately prior to the reduction of Ag on their surface in order to remove any surface contaminants.[28]

Core−Shell Synthesis. Au@Ag structures with a truncated octahedron geometry were formed by inserting substrate-supported templates into 1 mL of 10 mM ascorbic acid heated to 95 °C. After allowing 1 min for the substrate temperature to equilibrate, 3 mL of aqueous $AgNO_3$ (1 mM, 95 °C) was added in a dropwise manner over a 2.5 min interval. The reaction was then allowed to continue for a 4 min duration, after which the substrate was removed from the solution and sonicated in DI water for 30 s to remove spontaneously nucleated Ag nanoparticles from the substrate surface. Au@Ag structures with a cubic geometry were formed by first preparing 95 °C aqueous solutions of (i) 3 mL of 1 mM $AgNO_3$ and (ii) 1 mL of 10 mM trisodium citrate and 1 mL of 0.6 mM HNO_3. The substrate was then placed into the solution containing citrate, where it was allowed to equilibrate for 1 min. Cube formation was then initiated by rapidly adding the $AgNO_3$ solution and allowing the reaction to proceed for 5 min. The substrate was then removed from the solution and sonicated in DI water. Further details regarding this synthesis can be found elsewhere.[28]

Nanoshell, Nanocage, and Nanoframe Synthesis. Galvanic replacement reactions were carried out by inserting the substrate-supported Au@Ag into 3 mL of aqueous $HAuCl_4$ (20 μM) heated to 95 °C. The Au@Ag structures with the truncated octahedron geometry were typically reacted for 2, 6, and 10 min to obtain the nanoshell, nanocage, and nanoframe configurations, respectively. To obtain the same configurations for the Au@Ag structures with a cubic geometry required reaction times of 2, 6, and 12 min.

Optical Measurements. The extinction spectra shown in Figure 5 were measured using unpolarized light with an electric field (E) and propagation vector (k) parallel and perpendicular to the substrate surface, respectively. For both cases (*i.e.*, Au@Ag with a truncated octahedron and cubic geometry) a single sample was used to obtain all spectra. Obtaining this data, therefore, required that the sample be periodically removed from the liquid media containing reactants, rinsed in DI water, dried, characterized, and then reinserted into the reactants. Control experiments indicated that the removal and reinsertion process had no obvious influence on determining the reaction product.

Instrumentation. Template formation utilized a 681 Gatan high-resolution ion beam coater for film depositions and a Lindburg Blue M tube furnace for the dewetting procedure. An FEI 450 FEG ESEM was used to obtain SEM images and EDS maps and cross sections. The extinction spectra were obtained using a JASCO V-730 spectrometer.

ASSOCIATED CONTENT

Supporting Information

The Supporting Information is available free of charge on the ACS Publications website at DOI: 10.1021/acsnano.6b02712.

SEM images showing nanoshell porosity and nanoframes that have collapsed due to excessive galvanic replacement (PDF)

AUTHOR INFORMATION

Corresponding Author

*E-mail: neretina@temple.edu.

Notes

The authors declare no competing financial interest.

ACKNOWLEDGMENTS

This work is funded by a National Science Foundation award (DMR-1505114) to S.N. It has benefited from the facilities available through Temple University's Nano Instrumentation Center as well as the expertise of D. A. Dikin (Facility Manager). K.D.G. acknowledges support received through a Temple University Graduate Fellowship.

REFERENCES

(1) Xia, X.; Wang, Y.; Ruditskiy, A.; Xia, Y. 25th Anniversary Article: Galvanic Replacement: A Simple and Versatile Route to Hollow Nanostructures with Tunable and Well-Controlled Properties. *Adv. Mater.* **2013**, *25*, 6313−6333.

(2) Fang, Z.; Wang, Y.; Liu, C.; Chen, S.; Sang, W.; Wang, C.; Zeng, J. Rational Design of Metal Nanoframes for Catalysis and Plasmonics. *Small* **2015**, *11*, 25932605.

(3) Personick, M. L.; Mirkin, C. A. Making Sense of the Mayhem behind Shape Control in the Synthesis of Gold Nanoparticles. *J. Am. Chem. Soc.* **2013**, *135*, 18238−18247.

(4) Jones, M. R.; Osberg, K. D.; Macfarlane, R. J.; Langille, M. R.; Mirkin, C. A. Templated Techniques for the Synthesis and Assembly of Plasmonic Nanostructures. *Chem. Rev.* **2011**, *111*, 3736−3827.

(5) Xia, Y.; Xiong, Y.; Lim, B.; Skrabalak, S. E. Shape-Controlled Synthesis of Metal Nanocrystals: Simple Chemistry Meets Complex Physics? *Angew. Chem., Int. Ed.* **2009**, *48*, 60−103.

(6) Li, M.; Cushing, S. K.; Wu, N. Plasmon-Enhanced Optical Sensors: A Review. *Analyst* **2015**, *140*, 386−406.

(7) Wang, C.; Astruc, D. Nanogold Plasmonic Photocatalysis for Organic Synthesis and Clean Energy Conversion. *Chem. Soc. Rev.* **2014**, *43*, 7188−7216.

(8) Zeng, J.; Zhang, Q.; Chen, J.; Xia, Y. A Comparison Study of the Catalytic Properties of Au-Based Nanocages, Nanoboxes, and Nanoparticles. *Nano Lett.* **2010**, *10*, 30−35.

(9) Atwater, H. A.; Polman, A. Plasmonics for Improved Photovoltaic Devices. *Nat. Mater.* **2010**, *9*, 205−213.

(10) Yang, X.; Yang, M.; Pang, B.; Vara, M.; Xia, Y. Gold Nanomaterials at Work in Biomedicine. *Chem. Rev.* **2015**, *115*, 10410−10488.

(11) Ma, Y.; Li, W.; Cho, E. C.; Li, Z.; Yu, T.; Zeng, J.; Xie, Z.; Xia, Y. Au@Ag Core-Shell Nanocubes with Finely Tuned and Well-Controlled Sizes, Shell Thicknesses, and Optical Properties. *ACS Nano* **2010**, *4*, 6725−6734.

DOI: 10.1021/acsnano.6b02712
ACS Nano 2016, 10, 6354−6362

(12) Yang, Y.; Shi, J.; Kawamura, G.; Nogami, M. Preparation of Au-Ag, Ag-Au Core-Shell Bimetallic Nanoparticles for Surface-Enhanced Raman Scattering. *Scr. Mater.* **2008**, *58*, 862−865.
(13) Xia, Y.; Xia, X.; Peng, H.-C. Shape-Controlled Synthesis of Colloidal Metal Nanocrystals: Thermodynamic *versus* Kinetic Products. *J. Am. Chem. Soc.* **2015**, *137*, 7947−7966.
(14) Yang, Y.; Wang, W.; Li, X.; Chen, W.; Fan, N.; Zou, C.; Chen, X.; Xu, X.; Zhang, L.; Huang, S. Controlled Growth of Ag/Au Nanorods through Kinetics Control. *Chem. Mater.* **2013**, *25*, 34−41.
(15) Yang, Y.; Liu, J.; Fu, Z.-W.; Qin, D. Galvanic Replacement-Free Deposition of Au on Ag for Core-Shell Nanocubes with Enhanced Chemical Stability and SERS Activity. *J. Am. Chem. Soc.* **2014**, *136*, 8153−8156.
(16) Zeng, J.; Zheng, Y.; Rycenga, M.; Tao, J.; Li, Z.-Y.; Zhang, Q.; Zhu, Y.; Xia, Y. Controlling the Shapes of Silver Nanocrystals with Different Capping Agents. *J. Am. Chem. Soc.* **2010**, *132*, 8552−8553.
(17) Xia, Y. N.; Li, W. Y.; Cobley, C. M.; Chen, J. Y.; Xia, X. H.; Zhang, Q.; Yang, M. X.; Cho, E. C.; Brown, P. K. Gold Nanocages: From Synthesis to Theranostic Applications. *Acc. Chem. Res.* **2011**, *44*, 914−924.
(18) Lu, X.; Au, L.; McLellan, J.; Li, Z. Y.; Marquez, M.; Xia, Y. Fabrication of Cubic Nanocages and Nanoframes by Dealloying Au/Ag Alloy Nanoboxes with an Aqueous Etchant Based on $Fe(NO_3)_3$ or NH_4OH. *Nano Lett.* **2007**, *7*, 1764−1769.
(19) Xie, S.; Lu, N.; Xie, Z.; Wang, J.; Kim, M. J.; Xia, Y. Synthesis of Pd-Rh Core−Frame Concave Nanocubes and Their Conversion to Rh Cubic Nanoframes by Selective Etching of the Pd Cores. *Angew. Chem., Int. Ed.* **2012**, *51*, 10266−10270.
(20) Sun, Y.; Wiley, B.; Li, Z.-Y.; Xia, Y. Synthesis and Optical Properties of Nanorattles and Multiple-Walled Nanoshells/Nanotubes Made of Metal Alloys. *J. Am. Chem. Soc.* **2004**, *126*, 9399−9406.
(21) Cho, E. C.; Camargo, P. H. C.; Xia, Y. Synthesis and Characterization of Noble-Metal Nanostructures Containing Gold Nanorods in the Center. *Adv. Mater.* **2010**, *22*, 744−748.
(22) Khalavka, Y.; Becker, J.; Sönnichsen, C. Synthesis of Rod-Shaped Gold Nanorattles with Improved Plasmon Sensistivity and Catalytic Activity. *J. Am. Chem. Soc.* **2009**, *131*, 1871−1875.
(23) Kuai, L.; Wang, S.; Geng, B. Gold-Platinum Yolk-Shell Structure: A Facile Galvanic Displacement Synthesis and Highly Active Electrocatalytic Properties for Methanol Oxidation with Super CO-Tolerance. *Chem. Commun.* **2011**, *47*, 6093−6095.
(24) Gong, X.; Yang, Y.; Huang, S. A Novel-Selective Galvanic Reaction and Synthesis of Hollow Nanoparticles with an Alloy Core. *J. Phys. Chem. C* **2010**, *114*, 18073−18080.
(25) Xie, S.; Jin, M.; Tao, J.; Wang, Y.; Xie, Z.; Zhu, Y.; Xia, Y. Synthesis and Characterization of $Pd@M_xCu_{1-x}$ (M = Au, Pd, and Pt) Nanocages with Porous Walls and a Yolk-Shell Stucture through Galvanic Replacement. *Chem. - Eur. J.* **2012**, *18*, 14974−14980.
(26) Chen, H. M.; Liu, R.-S.; Asakura, K.; Lee, J.-F.; Lee; Jang, L.-Y.; Hu, S.-F. Fabrication of Nanorattles with Passive Shells. *J. Phys. Chem. B* **2006**, *110*, 19162−19167.
(27) Yang, J.; Lu, L.; Wang, H.; Zhang, H. Synthesis of Pt/Ag Bimetallic Nanorattle with Au Core. *Scr. Mater.* **2006**, *54*, 159−162.
(28) Hajfathalian, M.; Gilroy, K. D.; Hughes, R. A.; Neretina, S. Citrate-Induced Nanocubes: A Reexamination of the Role of Citrate As a Shape-Directing Capping Agent for Ag-Based Nanostructures. *Small* **2016**, DOI: 10.1002/smll.201600545.
(29) Gilroy, K. D.; Hughes, R. A.; Neretina, S. Kinetically Controlled Nucleation of Silver on Surfactant-Free Gold Seeds. *J. Am. Chem. Soc.* **2014**, *136*, 15337−15345.
(30) Gilroy, K. D.; Sundar, A.; Farzinpour, P.; Hughes, R. A.; Neretina, S. Mechanistic Study of Substrate-Based Galvanic Replacement Reactions. *Nano Res.* **2014**, *7*, 365−379.
(31) Gilroy, K. D.; Farzinpour, P.; Sundar, A.; Tan, T.; Hughes, R. A.; Neretina, S. Substrate-Based Galvanic Replacement Reactions carried out on Heteroepitaxially formed Silver Templates. *Nano Res.* **2013**, *6*, 418−428.
(32) Sundar, A.; Farzinpour, P.; Gilroy, K. D.; Tan, T.; Hughes, R. A.; Neretina, S. Eutectic Combinations As a Pathway to the Formation of Substrate-Based Au-Ge Heterodimers and Hollowed Au Nanocrescents with Tunable Optical Properties. *Small* **2014**, *10*, 3379−3388.
(33) Gilroy, K. D.; Farzinpour, P.; Sundar, A.; Hughes, R. A.; Neretina, S. Sacrificial Templates for Galvanic Replacement Reactions: Design Criteria for the Synthesis of Pure Pt Nanoshells with a Smooth Surface Morphology. *Chem. Mater.* **2014**, *26*, 3340−3347.
(34) Thompson, C. V. Solid-State Dewetting of Thin Films. *Annu. Rev. Mater. Res.* **2012**, *42*, 399−434.
(35) Henry, C. R. Morphology of Supported Nanoparticles. *Prog. Surf. Sci.* **2005**, *80*, 92−116.
(36) Sun, Y.; Xia, Y. Mechanistic Study on the Replacement Reaction between Silver Nanostructures and Chloroauric Acid in Aqueous Medium. *J. Am. Chem. Soc.* **2004**, *126*, 3892−3901.
(37) Goris, B.; Polavarapu, L.; Bals, S.; Tendeloo, G. V.; Liz-Marzán, L. M. Monitoring Galvanic Replacement Through Three-Dimensional Morphological and Chemical Mapping. *Nano Lett.* **2014**, *14*, 3220−3226.
(38) Sundar, A.; Farzinpour, P.; Gilroy, K. D.; Tan, T.; Hughes, R. A.; Neretina, S. Organized Surfaces of Highly Faceted Single-Crystal Palladium Structures Seeded by Sacrificial Templates. *Cryst. Growth Des.* **2013**, *13*, 3847−3851.
(39) Au, L.; Lu, X.; Xia, Y. A Comparative Study of Galvanic Replacement Reactions Involving Ag Nanocubes and $AuCl_2^-$ or $AuCl_4^-$. *Adv. Mater.* **2008**, *20*, 2517−2522.
(40) Zhang, A.-Q.; Qian, D.-J.; Chen, M. Simulated Optical Properties of Noble Metallic Nanopolyhedra with Different Shapes and Structures. *Eur. Phys. J. D* **2013**, *67*, 231.
(41) Yuan, L.; Zhu, J.; Ren, Y.; Bai, S. Sectional Area-Dependent Plasmonic Shifting in the Truncated Process of Silver Nanoparticles: From Cube to Octahedron. *J. Nanopart. Res.* **2011**, *13*, 6305−6312.
(42) Olson, T. Y.; Schwartzberg, A. M.; Orme, C. A.; Talley, C. E.; O'Connell, B.; Zhang, J. Z. Hollow Gold-Silver Double-Shell Nanospheres: Structure, Optical Absorption, and Surface-Enhanced Raman Scattering. *J. Phys. Chem. C* **2008**, *112*, 6319−6329.
(43) Ma, Y.-W.; Zhang, L.-H.; Wu, Z.-W.; Yi, M.-F.; Zhang, J.; Jian, G.-S. The Study of Tunable Local Surface Plasmon Resonances on Au-Ag and Ag-Au Core-Shell Alloy Nanostructure Particles with DDA Method. *Plasmonics* **2015**, *10*, 1791−1800.
(44) Mahmoud, M. A.; El-Sayed, M. A. Substrate Effect on Plasmonic Sensing Ability of Hollow Nanoparticles of Different Shapes. *J. Phys. Chem. B* **2013**, *117*, 4468−4477.
(45) Priebe, M.; Fromm, K. M. Nanorattles or Yolk-Shell Nanoparticles − What Are They, How Are They Made, and What Are They Good For. *Chem. - Eur. J.* **2015**, *21*, 3854−3874.
(46) Lee, J.; Kim, S. M.; Lee, I. S. Functionalization of Hollow Nanoparticles for Nanoreactor Applications. *Nano Today* **2014**, *9*, 631−667.
(47) Li, G.; Tang, Z. Noble Metal Nanoparticle@Metal Oxide Core/Yolk-Shell Nanostructures As Catalysts: Recent Progress and Perspective. *Nanoscale* **2014**, *6*, 3995−4011.
(48) Fang, X.; Liu, Z.; Hsieh, M.-F.; Chen, M.; Liu, P.; Chen, C.; Zheng, N. Hollow Mesoporous Aluminosilica Sphere with Perpendicular Pore Channels As Catalytic Nanoreactors. *ACS Nano* **2012**, *6*, 4034−4444.
(49) Yang, Y.; Liu, X.; Li, X.; Zhao, J.; Bai, S.; Liu, J.; Yang, Q. A Yolk-Shell Nanoreactor with a Basic Core and an Acid Shell for Cascade Reactions. *Angew. Chem., Int. Ed.* **2012**, *51*, 9164−9168.
(50) Zhang, X.; Chen, Y. L.; Liu, R.-S.; Tsai, D. P. Plasmonic Photocatalysis. *Rep. Prog. Phys.* **2013**, *76*, 046401.
(51) Linic, S.; Aslam, U.; Boerigter, C.; Morabito, M. Photochemical Transformations on Plasmonic Metal Nanoparticles. *Nat. Mater.* **2015**, *14*, 567−576.
(52) Rycenga, M.; Cobley, C. M.; Zeng, J.; Li, W.; Moran, C. H.; Zhang, Q.; Qin, D.; Xia, Y. Controlling the Synthesis and Assembly of Silver Nanostructures for Plasmonic Applications. *Chem. Rev.* **2011**, *111*, 3669−3712.
(53) Liu, G.; Zhang, C.; Wu, J.; Mirkin, C. A. Using Scanning-Probe Block Copolymer Lithography and Electron Microscopy to Track

DOI: 10.1021/acsnano.6b02712
ACS Nano 2016, 10, 6354−6362

Shape Evolution in Multimetallic Nanoclusters. *ACS Nano* **2015**, *9*, 12137−12145.
(54) Cha, S. K.; Mun, J. H.; Chang, T.; Kim, S. Y.; Kim, J. Y.; Jin, H. M.; Lee, J. Y.; Shin, J.; Kim, K. H.; Kim, S. O. Au−Ag Core−Shell Nanoparticle Array by Block Copolymer Lithography for Synergistic Broadband Plasmonic Properties. *ACS Nano* **2015**, *9*, 5536−5543.
(55) Farzinpour, P.; Sundar, A.; Gilroy, K. D.; Eskin, Z. E.; Hughes, R. A.; Neretina, S. Altering the Dewetting Characteristics of Ultrathin Gold and Silver Films using a Sacrificial Antimony Layer. *Nanotechnology* **2012**, *23*, 495604.
(56) Farzinpour, P.; Sundar, A.; Gilroy, K. D.; Eskin, Z. E.; Hughes, R. A.; Neretina, S. Dynamic Templating: A Large Area Processing Route for the Assembly of Periodic Arrays of Sub-Micrometer and Nanoscale Structures. *Nanoscale* **2013**, *5*, 1929−1938.

DOI: 10.1021/acsnano.6b02712
ACS Nano 2016, 10, 6354−6362